# Searching for the helical-gradient force on chiral molecules

J.A. Jones, B. Regan, J. Painter, J. Mills, I. Dutta, B. Khajavi, and E.J. Galvez

Department of Physics and Astronomy, Colgate University, Hamilton, NY 13346, U.S.A.

## ABSTRACT

We investigate a force that has been predicted to discriminate molecules by their chirality when they are in the presence of an optical field with a polarization-helicity gradient. We investigate several experimental geometries for observing evidence of this force via enantiometer separation in racemic mixtures. We do this with singular-optical beams carrying a polarization helicity gradient across their transverse mode. Molecular diffusion and the dipole force – an intensity-gradient force – have so far precluded measurements of this force.

**Keywords:** Polarization, Chirality

## 1. INTRODUCTION

It is well known that in living organisms there is a preference towards molecular chirality. For example, DNA and sugars are right-handed, whereas proteins and amino acids are left-handed. Chiral molecules interact distinctly with cells and other living organisms. A vivid example is the scent of oranges and lemons: they appear distinct to the olfactory system, yet they involve mirror copies (enantiometers) of the same molecule, limonene. The different enantiometers attach to distinct groups of olfactory receptors, resulting in the different sensory reactions. In pharmaceuticals the effect of molecules can have hugely distinct consequences depending on the molecular chirality.[1] The most notorious but unfortunate case is that of thalidomide, which was prescribed to pregnant women in the 1950's due the sedative effects of its right-handed isomer, in ignorance that its left-handed enantiometer also present in the medicine produced birth defects. In methorphan, one enantiomer, dextromethorphan, is a common cough relief drug found in flu and cold syrups, whereas its mirror image, levomethorphan, is a schedule II narcotic in the United States, behaving as an opiod. In other cases the enantiometers of pharmaceuticals are benign, as in the case of ibuprofen, and so it is sold as a racemic mixture of both enantiomers (i.e., equal mixture of both right- and left-handed ibuprofen molecules). Thus, chirality is very important in pharmaceuticals, where more than 50% of pharmaceuticals are chiral.

Chiral isomers interact with light in a peculiar way. The distinct chiralities are optically active, rotating the polarization of the light in a direction that depends on the chirality. It is a type of light/matter phenomenon that depends on the interactions of molecules with both the electric and magnetic components of the light. One classification of chiral molecules is based on how they rotate linearly polarized light: levo- and dextro- rotatory. These definitions are not necessarily tied to the geometric distribution of atoms in the chiral isomers, classified as R- (rectus) and S- (sinister).

In the last few years two independent theoretical treatments, one quantum mechanical[2,3] and another one classical[4–6] have predicted a new type of light-matter interaction that discriminates between chiral enantiometers. The phenomenon is based on the same principles as optical activity: light scattering. It involves the interaction of a molecule with the gradient of helicity of the light field. In such an environment, the molecule experiences a force that depends on the molecular properties and the gradient in the helicity of the light. The sign of the force depends on the chirality of the molecule. Thus, it could provide a new way to separate enantiometers. In this article we present our recent attempts at measuring evidence of this helicity-gradient interaction on chiral molecules.

Further author information: (Send correspondence to E.J.G.)
E.J.G.: E-mail: egalvez@colgate.edu, Telephone: 1 315 228 7205
Proceedings of SPIE **10120**, (2017).

## 2. BACKGROUND

It has been proposed that the force that a chiral molecule experiences due to a light field is given by[2,4]

$$\mathbf{F} = a\nabla w + b\nabla h, \tag{1}$$

where $w$ and $h$ are the local electric energy density and the local helicity density of the optical field, respectively. The coefficients $a$ and $b$ are molecule-dependent constants, but $a$ is the same sign for both enantiomers whereas $b$ is of opposite sign for the two enantiomers. Therefore, if the gradient of the electric energy density across the optical field is constant, then a spatially variable helicity will generate an optical force that discriminates molecules by their chirality.

### 2.1 The Helicity

We define the basis states of right and left circular polarization as $\hat{e}_R$ and $\hat{e}_L$, respectively, in terms of the cartesian basis:

$$\hat{e}_R = \frac{1}{\sqrt{2}}\left(\hat{e}_x - i\hat{e}_y\right) \tag{2}$$

and

$$\hat{e}_L = \frac{1}{\sqrt{2}}\left(\hat{e}_x + i\hat{e}_y\right), \tag{3}$$

and define the general expressions of the electric and magnetic field of light in terms of them:

$$\mathbf{E} = E_0\left(\cos\chi\,\hat{e}_R + \sin\chi e^{i\gamma}\,\hat{e}_L\right) \tag{4}$$

and

$$\mathbf{B} = \frac{iE_0}{c}\left(\cos\chi\,\hat{e}_R + \sin\chi e^{i\gamma}\,\hat{e}_L\right), \tag{5}$$

where $\chi$ determines the ratio of amplitudes of the left- and right-circular components and $\gamma$ is the phase difference between the two components. The helicity is defined as[4]

$$h = \frac{\epsilon_0 c}{2}(\mathbf{A}\cdot\mathbf{B} - \mathbf{C}\cdot\mathbf{E}), \tag{6}$$

where $\mathbf{A}$ is the magnetic vector potential and $\mathbf{C}$ is the electric pseudovector potential. They are related to the electric and magnetic fields by

$$\mathbf{E} = -\frac{\partial\mathbf{A}}{\partial t} = -\frac{1}{\epsilon_0\mu_0}\left(\nabla\times\mathbf{C}\right) \tag{7}$$

and

$$\mathbf{B} = \nabla\times\mathbf{A} = -\frac{\partial\mathbf{C}}{\partial t}. \tag{8}$$

Replacing the fields in Eqs. 4 and 5 yields

$$\mathbf{A} = \frac{-iE_0}{\omega}\left(\cos\chi\,\hat{e}_R + \sin\chi e^{i\gamma}\,\hat{e}_L\right) \tag{9}$$

and

$$\mathbf{C} = \frac{E_0}{\omega c}\left(\cos\chi\,\hat{e}_R - \sin\chi e^{i\gamma}\,\hat{e}_L\right), \tag{10}$$

and the helicity becomes

$$h = \frac{\epsilon_0 E_0^2}{\omega}\left(\cos^2\chi - \sin^2\chi\right) \tag{11}$$

$$= \frac{\epsilon_0 E_0^2}{\omega}\left(\cos 2\chi\right) \tag{12}$$

$$= \frac{\epsilon_0 E_0^2 s_3}{\omega}. \tag{13}$$

where $s_3 = \cos 2\chi$ is one of the normalized Stokes parameters. The ellipticity of the field, defined as the ratio of the semi-minor ($b$) to semi-major ($a$) axes of the polarization ellipse, is related to $s_3$ by

$$\epsilon = \frac{b}{a} = \frac{1 - \sqrt{1 - s_3^2}}{s_3}. \tag{14}$$

The helicity gradient is then given by

$$\frac{dh}{dx} = -\frac{2\epsilon_0 E_0^2}{\omega} \sin\chi \frac{d\chi}{dx}. \tag{15}$$

### 2.2 Optical field

To isolate the helicity-gradient force in Eq. 1 we require constant electric field density. In our previous research[7] we have investigated space-variant polarization patterns that can have a uniform intensity but with a helicity gradient. We use a superposition of Laguerre-Gauss (LG) beams given by

$$\mathbf{E} = \frac{E_0}{2}\left(LG_0^{+1}\hat{e}_V + LG_0^0\hat{e}_H\right), \tag{16}$$

where the LG mode is expressed in transverse coordinates $(r, \phi)$ by

$$LG_0^\ell = A_\ell r^\ell e^{i\ell\phi} e^{-r^2/w^2}, \tag{17}$$

and having topological charge $\ell$ where $w$ is the mode half-width, and coefficients $A_0 = \sqrt{2}/(\sqrt{\pi}w)$ and $A_1 = 2/(\sqrt{\pi}w^2)$. This superposition of LG beams is also referred to as a Poincaré beam, which has spatially-variable polarization. The Poincaré beam contains a mapping of all polarizations on the surface of the Poincaré sphere. The modeled and measured polarization patterns of this beam are shown in Figs. 1(a) and (b), respectively. The false color in the figures encodes the Stokes parameter $s_3$. The modeled and the measured beam are in good agreement; we were able to create this beam as described in Sec. 3. The pattern has two-circular polarization singularities (C-points) of left and right handedness, as shown in Figs. 1(a) and 1(b). The polarization of the light changes ellipticity from one C-point to the other.

In Fig. 1(c) we plot the calculated and measured normalized Stokes parameter $s_3$ along the line that connects the two C-points. As can be seen, the graph of $s_3$ shows a helicity gradient along this line.The 2-dimensional gradient is also evident by the color coding (online) of Figs. 1(a) and 1(b). The experimental measurements show a very good agreement of the measured gradient with the expectation, although some beam-mode imperfections conspire against an agreement throughout the beam profile. Figure 1c also shows a plot of the modeled intensity along the line connecting the two C-Points. The model using ideal modes gives nearly constant intensity along positions where we see a maximum change in $s_3$. The actual measurements show fluctuations that are due to imperfections in the beam mode.

By replacing the expressions for the modes used, and using $\delta = \pi/2$, we get

$$\tan\chi = \frac{|A_1(x+iy) - A_0|}{|A_1(x+iy) + A_0|}. \tag{18}$$

If we fix $y = 0$ (the line passing through the C-points), we get

$$\chi = \tan^{-1}\left(\frac{ax-1}{ax+1}\right), \tag{19}$$

where $a = \sqrt{2}/w$. We used this expression in the modeling of $s_3$ along the line connecting the C-points in Fig. 1. Using the previous expression we obtain the helicity gradient:

$$\frac{d\chi}{dx} = \frac{(\sqrt{2}/w)}{2x^2/w^2 + 1}. \tag{20}$$

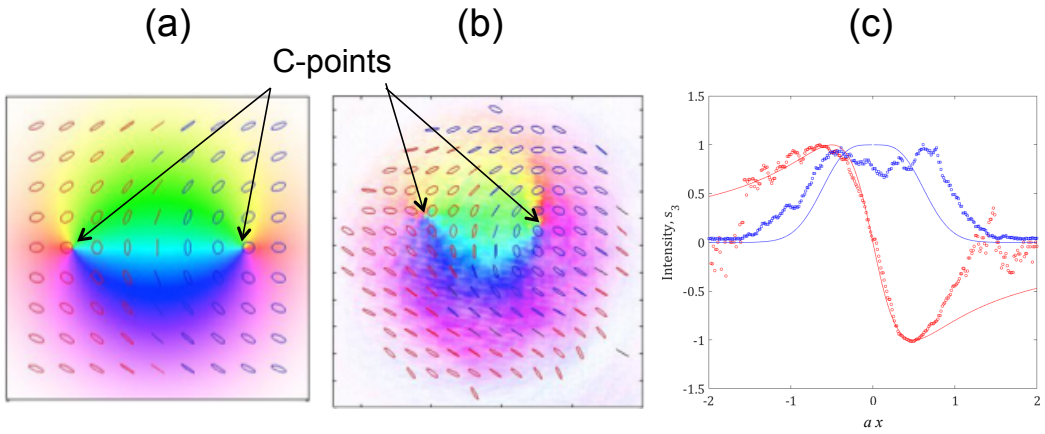


Figure 1. Polarization maps of the computationally modeled (a), and measured (b), Poincaré beam. The false color encodes the value of the Stokes parameter $s_3$. The left- and right-handed C-point singularities are shown. In (c), the normalized Stokes $s_3$ parameter (red) and intensity (blue) of the modeled (line) and measured (symbols) Poincaré beam are plotted with respect to the radial position relative to the mode half-width ($a = \sqrt{2}/w$).

The maximum gradient is at $x = 0$, then noting that $\sin 2\chi = -1$ we get:

$$\frac{dh}{dx}|_{\max} = \frac{2\sqrt{2}\epsilon_0 E_0^2}{\omega w}. \tag{21}$$

We can put the electric field of the light in terms of measurable quantities, such as the total power of the beam of light $P$ (expressed in W) or the irradiance $I_0$ (expressed in W/m$^2$). The irradiance can be expressed as

$$I_0 = \frac{\epsilon_0 c|\mathbf{E}|^2}{2} \tag{22}$$

Because we have a superposition of two beams (Eq. 16), the irradiance for this problem is given by

$$I_0 = \frac{c\epsilon_0 E_0^2}{4}\left(A_\ell^2 r^2 e^{-2r^2/w^2} + A_0^2 e^{-2r^2/w^2}\right) \tag{23}$$

$$= \frac{c\epsilon_0 E_0^2}{4}\left(\frac{2r^2}{w^2} + 1\right) e^{-2r^2/w^2} \tag{24}$$

Since

$$P = \int_0^\infty 2\pi r I_0 dr. \tag{25}$$

then integrating we obtain

$$P = \frac{c\epsilon_0 \pi w^2 E_0^2}{4} \tag{26}$$

or

$$E_0^2 = \frac{4P}{c\epsilon_0 \pi w^2}, \tag{27}$$

which replacing into Eq. 21 yields

$$\frac{dh}{dx}|_{\max} = \frac{8\sqrt{2}P}{\omega w^3 c\pi}. \tag{28}$$

Just to give some numerical estimate, If we consider visible (488 nm) light with power $P = 0.1$ W, with a half width of 0.1 mm we get a gradient $dh/dx|_{\max} = 3 \times 10^{-13}$ N s m$^{-3}$.

## 2.3 Optical Activity

Chirality is an intrinsic property of any molecule that has more than 4 atoms in it. These atoms can arrange into two or more different stereoisomers, or molecules with the same chemical formula: same atom to atom linkages and bonding distances but different three-dimensional arrangement. Chiral enantiometers are mirror images of each other, and so they are non-superimposable. The classic example is our hands: they are mirrors of each other, but when you compare them side by side to match finger by finger, the palms face opposite directions.

Chiral enantiometers have the same physical and chemical properties but interact differently with organic matter. When two enantiometers of concentration $E_1$ and $E_2$ are in a solution, the enantiometer excess is defined as

$$e.e. = \frac{|E_1 - E_2|}{E_1 + E_2}. \tag{29}$$

This quantity is usually expressed as a percentage. A racemic mixture contains equal amounts of both enantiometers, and so $e.e. = 0$.

This phenomenon involves a medium with an intrinsic chirality. It is either composed of chiral molecules embedded in a medium (solid, liquid or gas), or a solid with an intrinsic structural chirality. An optically active medium rotates the orientation of the polarization ellipse of an incoming electromagnetic wave. Alternatively, since the orientation can be understood as a relative phase between the right and left circularly polarized components of the light, an optically active medium can be understood as having two distinct indices of refraction for the circular polarization components of the light.

Operationally, the rotation of the orientation of the polarization due to a liquid medium containing a pure enantiometric solution of chiral molecules is given by

$$\alpha_e = l\ [c]\ [\alpha] \tag{30}$$

where $l$ is the length of the medium (usually expressed in dm), $[c]$ the concentration of the chiral molecules in the medium (usually expressed in g/cm$^3$), and $[\alpha]$ is the specific rotation of the molecule (usually expressed in degrees per dm g/cm$^3$). Table 1 shows parameters for a variety of molecules.

Table 1. Specific rotations of chiral molecules and their mass.

| Molecule | Specific Rotation (°) | Mol. Mass (amu) |
|---|---|---|
| DL Tartaric acid | 12.4 | 150.1 |
| Bi-naphtol | 30.1 | 286.3 |
| Carvone | 61 | 150.2 |
| Limonene | 115 | 136.2 |
| Quinine | 127 | 324.4 |
| Penicillin V | 223 | 350.4 |
| 4-helicene | 1670 | 256.1 |
| 6-helicene | 3750 | 328.4 |
| 14-Helicene | 7401 | 728.9 |

The rotation for a given enantiometric excess is given by

$$\alpha = \alpha_e(e.e.). \tag{31}$$

One of the molecules that we use in our experiment is Bi-naphtol (BINOL). For an experimental technique that detects a minimum rotation $\alpha_{\min}$, the minimum detectable enantiometric excess is then

$$(e.e.)_{\min} = \frac{\alpha_{\min}}{\alpha_e}. \tag{32}$$

The constant $b$ of Eq. 1 is given by[5]

$$b = \frac{\omega G'}{3\epsilon_0 c}, \tag{33}$$

where the constant $G'$ has equal magnitude but opposite sign for the enantiometers of the molecule. It is related to the specific rotation by[5]

$$G' = \frac{3\epsilon_0 c^2 \pi \omega^2 M[\alpha]}{6000(n^2+2)\omega_0^2}, \tag{34}$$

where $\omega_0$ is the angular frequency for which the specific rotation is defined, $M$ is the molecular mass, $n$ is the index of refraction of the medium, and $[\alpha]$ is the specific rotation of the molecule (next section).Thus, one way to search for potential ways to gauge the size of the force is through the optical activity of the molecule. For binaphtol and hexahelicene (data below) we get respectively $G'_{\text{Binaphtol}} = 4.6 \times 10^{-21}$ m kg$^{-1}$ s$^3$ A$^2$ and $G'_{\text{Hexah}} = 7.2 \times 10^{-19}$ m kg$^{-1}$ s$^3$ A$^2$, resulting in $b_{\text{Binaphtol}} = \omega G'/(3\epsilon_0 c) = 5.8 \times 10^{-19}$ m$^3$ s$^{-1}$ and $b_{\text{Hexah}} = \omega G'/(3\epsilon_0 c) = 9.1 \times 10^{-17}$ m$^3$ s$^{-1}$.

## 3. EXPERIMENTAL METHODS

In our quest to observe the proposed helicity-gradient force, we utilized several experimental geometries. The schematics of our experiments are shown in Figs. 2 and 3. The light source was a vertically polarized output beam of an argon-ion laser with a wavelength of 488 nm. The laser output was a fundamental Gaussian mode, also known as an LG beam of topological charge $\ell = 0$. This beam was directed to a Mach-Zehnder type interferometer. In one arm of the interferometer the polarization of the $\ell = 0$ beam was rotated to horizontal using a half-wave plate (HWP). In the other arm, the beam passed through a spiral phase plate (SPP) to generate an LG beam with topological charge $\ell = 1$. Upon exiting the interferometer, the horizontally polarized $\ell = 0$ beam was combined with the $\ell = 1$ beam to generate a Poincaré beam with the desired helicity gradient.

The Poincaré beam was guided through the sample cell by dichroic mirrors. The sample cell contained a racemic mixture of chiral molecules in solution. We used two racemic solutions: 0.40 g of BINOL dissolved in 30mL of ethanol or 4.5 g of racemic tartaric acid dissolved in 30 mL of deionized water. We used commercial cylindrical cells of several lengths and radii made of BK7 glass. The second output of the interferometer was sent through a polarizer and to a screen for diagnosis.

### 3.1 Description of detection methods

We utilized two optical methods to observe evidence of the helical-gradient force. One method, shown in Fig. 2, consisted of using a counter-propagating linearly polarized HeNe beam (632.8 nm). The transmission axis of a polarizer placed after the sample cell, as shown in Fig. 2, was adjusted to extinguish the probe beam when the pump beam did not go through the sample. When the sample has a racemic mixture, the net effect is no polarization rotation of linearly polarized light. When the pump beam was on, any enantiomer imbalance along the beam path would result in some of the probe beam being transmitted through the polarizer. The greater the excess along the probe beam path, the more polarization rotation the probe beam experiences. The probe beam continued into a detector. To increase the sensitivity, we modulated the phase between the two arms of the interferometer using a piezo-electric. This modulation changed the sign of the helicity gradient.

The second method of optical detection involved sending two displaced probe beams through the cell. These two beams were prepared by sending the HeNe laser through a beam-splitter-mirror pair as shown in Fig. 3. A quarter-wave plate prepared both beams in the same state of circular polarization. One of the probe beams overlapped with the counter-propagating pump beam. The other probe beam passed near the edge of the sample cell. They were sent together through the sample cell, one through the active region where the pump beam was present, and the other near the edge of the sample cell (not overlapping with the beam with the helicity-gradient). After passing through the sample cell, the beams were recombined and sent to a screen and an interference pattern was measured. We used a piezo-electric to modulate the sign of the helicity-gradient as mentioned earlier. An enantiometer excess in one of the probe beams would change the phase of the circularly polarized light, which would manifest in fringe shift. The probe beam that does not overlap with the pump beam served as a reference beam, assuming that any helicity-gradient force would not affect it.

The previous two methods used optical beams that were expanded to a beam spot of 5 mm. Then we also did similar type of experiments with focused beams and a shorter cell.

### 3.2 Imaging polarimetry

After passing through the sample cell of BINOL in ethanol solution, the light beam then passed through a quarter-wave plate (QWP) and a polarizer (Pol) that filtered the light in any of six basis polarization states, vertical (V), horizontal (H), diagonal (D), anti-diagonal (A), right-circular (R), or left-circular (L). The images of the probe beam after passing through the polarization filter were collected with a digital camera and were analyzed using a MATLAB program to determine the Stokes for each imaged point.

In polarimetry, the Stokes parameters are obtained by:

$$S_0 = I_{\rm H} + I_{\rm V} \tag{35}$$
$$S_1 = I_{\rm H} - I_{\rm V} \tag{36}$$
$$S_2 = I_{\rm D} - I_{\rm A} \tag{37}$$
$$S_3 = I_{\rm R} - I_{\rm L} \tag{38}$$

Where $I_{\rm H}$, $I_{\rm V}$, $I_{\rm D}$, $I_{\rm A}$, $I_{\rm R}$ and $I_{\rm L}$ are the intensities measured with the filters H, V, D, A, R and L, respectively. The normalized Stokes parameters are defined by $s_i = S_i/S_0$ $(i = 0, 1, 2, 3)$. The ellipticity of polarized light is as defined in Eq. 14. The orientation of the semi-major axis of the polarization ellipse is defined from horizontal as

$$\theta = \frac{1}{2}\tan^{-1}\left(\frac{s_2}{s_1}\right). \tag{39}$$

We used this imaging polarimetry technique to determine how the polarization of the probe beam changes across the sample (a mapping similar to the one shown in Fig. 1). For this case, the probe beam was made to be larger

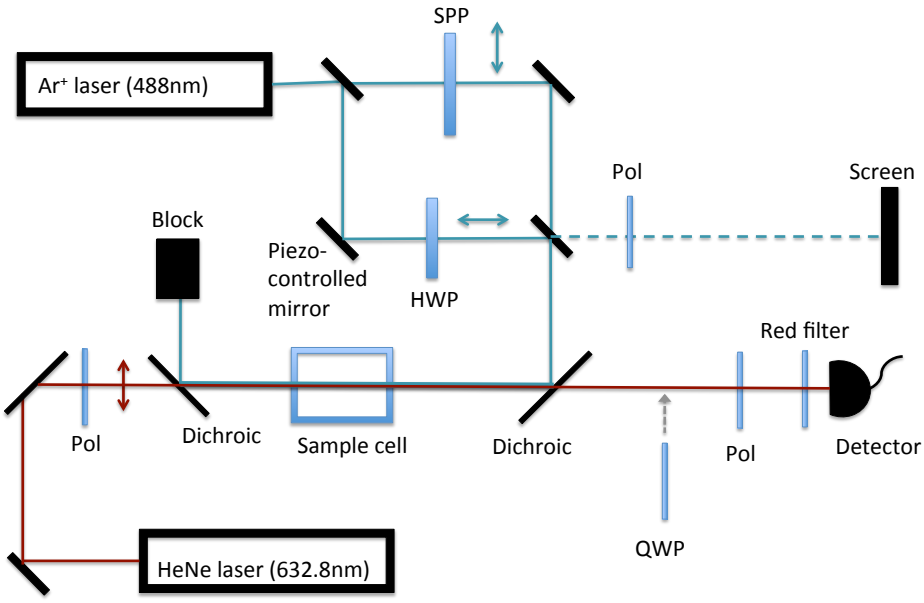


Figure 2. Experimental setup using the detection of polarization of probe beam. This setup utilizes either an intensity meter or a camera as the detector. When using the camera, a quarter-wave plate (QWP) is introduced to perform imaging polarimetry on the HeNe probe beam. Other components included polarizers (Pol), half-wave plates (HWP) and spiral phase plate (SPP).

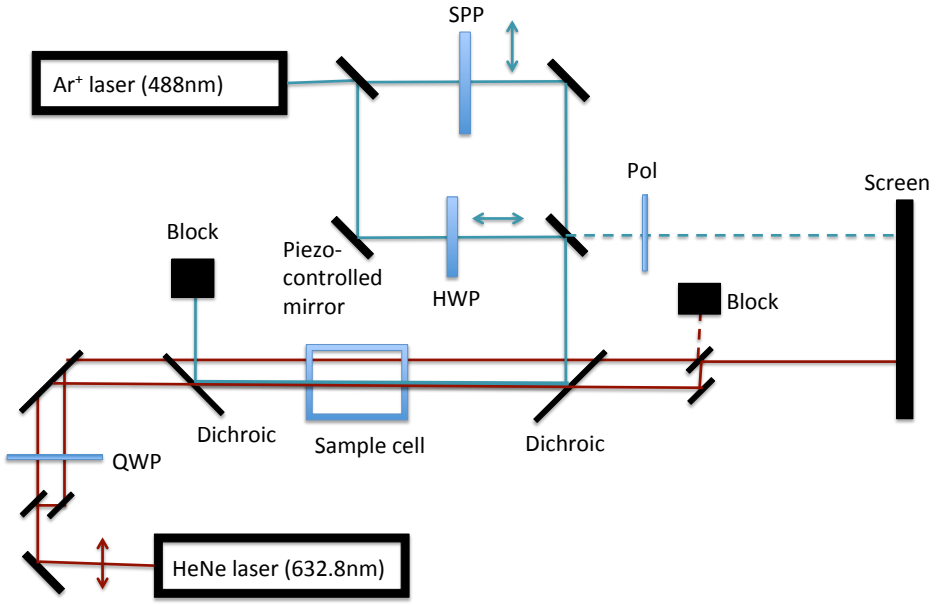


Figure 3. Adaptation to experimental setup to detect changes in phase between two circularly-polarized probe beams after passing through different areas of the sample cell. Interference fringes are observed on a screen.

in diameter than the pump beam. Therefore, the probe beam should give information about the distribution of an entiomeric excess along the helicity-gradient, outside of the pump beam area, and transverse to the helicity gradient.

## 4. RESULTS

Although our measurements are ongoing, to this point, helicity-gradient force effects have given null results so far. With the first geometry we found it difficult to prevent changes in intensity as the helicity was modulated. This was verified by independent checks in the apparatus. In that geometry the pump beam was expanded to fill the cross section of the cell. This diminished the gradient force. Using the parameters given by the theory, we calculated that under this circumstances (BINOL with expanded beam) the helicity gradient force was of the order of $10^{-21}$ N. As mentioned below, this value is much too small compared to diffusion effects, estimated to be a few orders of magnitude greater.

Our second attempt reduced the diameter of the beam significantly, and even focused the beam. Under such circumstances the pump beam created a significant intensity-gradient force that changed the local concentration of molecules in the solvent. This produced a refractive-index gradient in the cell, which in turn would significantly defocus the probe beam. These experiments allowed us to get estimates of the diffusion time, of the order of 1-2 s.

### 4.1 Diffusion

Diffusion competes with the effects of the helicity-gradient force. When the pump beam was focused the effect of diffusion was most visible, because it expanded the probe beam significantly.

We made a number of simplifying assumptions to estimate the time-effect of diffusion. First, the interaction region was much smaller in diameter than the sample cell. The beam diameter is approximately 60 $\mu$m and the sample cell is approximately 2 cm. We assumed that the supply of new molecules is infinite. Second, because the helicity-gradient force is 1-dimensional, then the concentration gradient is also 1-dimensional for our

diffusion model. Third, estimates suggest that a concentration gradient of approximately 5 per cent is achievable by applying the helicity-gradient force. For simplicity, we assumed that at the edge of the pump beam the concentration is 5 per cent greater than inside the beam. Due to the larger concentration directly outside of the pump beam, we assumed that there is an effective barrier to the diffusing molecules; i.e., that the preference of the molecules is to diffuse back into the beam where there is a lower concentration rather than further away from the beam. It is only this 5 per cent concentration excess that we consider to be diffusing. Fourth, we assumed that due to symmetry that the diffusion effects from one edge of the beam to the center is identical to the diffusion effects from the opposite edge of the beam to the center. Therefore, we are considering diffusion from the edge of the beam to the center, equal to the beam waist (approximately 30 $\mu m$).

Considering the above simplifying assumptions, we used a simple Fickian diffusion model with molecules diffusing with a barrier at $x = 0^-$ in the positive $x$-direction in a Cartesian coordinate system[8]

$$J(x,t) = \frac{1}{2}\frac{x}{t}\left(\frac{N^2}{4\pi Dt}\right)^2 e^{-x^2/4Dt}, \tag{40}$$

where $J(x,t)$ is the diffusion rate in moles $\mathrm{m}^{-2}\ \mathrm{s}^{-1}$, $N$ is the number of molecules, and $D$ is the diffusion constant for the molecule in solution. To determine a value for $N$, we used the properties and conditions of the sample cell containing BINOL

$$N_{\mathrm{BINOL}} = \left(\frac{6.02\times 10^{23}\mathrm{molecules}}{286\mathrm{g}}\right)(0.4\mathrm{g}) = 8\times 10^{20}\mathrm{molecules}. \tag{41}$$

Lastly, for the diffusion constant $D$ we used an order-of-magnitude estimate of $10^{-10}\mathrm{m}^2/\mathrm{s}$. Using these estimates, diffusion occurs on the order of seconds. This estimate is in good agreement with the observed time evolution of the fringe pattern when the pump beam is suddenly turned off. The fringe pattern returns to the "pump off" state on the order of a few seconds.

## 5. CONCLUSIONS

Our conclusion thus far is a null result. There are numerous effects that compete with the helicity-gradient force. Most noticeably, our observations of the fringe patterns in the interference analysis seem to be dominated by laser-intensity effects. The work presented here includes our first attempts to observe the proposed enantiomer dependent helicity-gradient force on chiral molecules.

## ACKNOWLEDGMENTS

This work was funded by NSF grant PHY-1506321. We thank David Andrews, Robert Cameron, and Anthony Chianese for useful discussions.

## REFERENCES

[1] Smith, S. W., "Chiral toxicology: It's the same thing... only different," *Toxicological Sciences* **110**(1), 4–30 (2009).
[2] Bradshaw, D. S. and Andrews, D. L., "Chiral discrimination in optical trapping and manipulation," *New J. Phys.* **16**, 103021 1–16 (2014).
[3] Bradshaw, D. S. and Andrews, D. L., "Laser optical separation of chiral molecules," *Opt. Lett.* **40**, 677–680 (2015).
[4] Cameron, R. P., Barnett, S. M., and Yao, A. M., "Discriminatory optical force for chiral molecules," *New J. Phys.* **16**, 013020 (2014).
[5] Cameron, R. P., Yao, A. M., and Barnett, S. M., "Diffraction gratings for chiral molecules and their applications," *J. Phys. Chem.* **118**, 3472–3478 (2014).
[6] Canaguier-Durand, A., Hutchison, J. A., Genet, C., and Ebbesen, T. W., "Mechanical separation of chiral dipoles by chiral light," *New. J. Phys.* **15**, 123037 (2013).
[7] Galvez, E., Khadka, S., Schubert, W., and Nomoto, S., "Poincaré-beam patterns produced by non-separable superpositions of Laguerre-Gauss and polarization modes of light," *Appl. Opt.* **51**, 2925–2934 (2012).
[8] Gillespie, D. T. and Seitaridou, E., [*Simple Brownian Diffusion*], Oxford University Press (2013).